JOURNAL OF AIRCRAFT
Vol. 36, No. 4, July–August 1999

Further Convergence Studies of the Enhanced Doublet-Lattice Method

William P. Rodden*
William P. Rodden, Ph.D., Inc., La Cañada Flintridge, California 91011
Paul F. Taylor†
Gulfstream Aerospace Corporation, Savannah, Georgia 31402
Samuel C. McIntosh Jr.‡
McIntosh Structural Dynamics, Inc., Palo Alto, California 94306
and
Myles L. Baker§
The Boeing Company, Long Beach, California 90807

The doublet-lattice method (DLM) has become a standard source for the aerodynamic loads in flutter and dynamic response analyses of aircraft at subsonic speeds. A recent refinement to the method is based on an improvement to the integration of the oscillatory kernel function by replacing the parabolic approximation in the kernel numerator with a more accurate quartic approximation. This refinement extends the frequency limits of the DLM for applications to higher-frequency flutter and dynamic response. The effects of Mach number and lattice geometry on convergence by numerical experimentation with some previously studied configurations are reviewed as well as a realistic aircraft model, present guidelines are reviewed, and updated guidelines for box aspect ratio and number of boxes per wavelength are presented.

Introduction

THE doublet-lattice method (DLM) is a finite-element method for the solution of the oscillatory subsonic pressure-normalwash integral equation for multiple interfering lifting surfaces. Since its first appearance,[1] it has had two significant refinements.[2,3] In the later refinement more accurate approximations (quartics) were made to the numerator of the incremental kernel for the oscillatory normalwash factors in the pressure-normalwash matrix equation. The new normalwash factors were developed, and a computer program called N5KQ (based on the computer program N5KA of Ref. 4) was utilized to demonstrate the improved accuracy of the new formulation over the previous parabolic approximations used in the earlier-refined DLM.[2] Applications were made to rigid planar and nonplanar configurations for limited reduced frequency and Mach number combinations to determine an increased limit for the permissible aspect ratio (AR) of the lifting elements (boxes) in the lifting-surface finite-element idealization, which was tentatively estimated at 5 or 6, a significant increase over the value of 3, the guideline recommended in Ref. 5.

The applications in Ref. 3 followed the guideline in Ref. 5 for the DLM that recommended that the aerodynamic idealization have more than $N_\lambda = 12$ box chords for the minimum wavelength of the motion. The wavelength λ depends on the reduced frequency k_r and its reference length $\bar{c}$,

$$\lambda = \pi \bar{c}/k_r \tag{1}$$

and the box chord Δx should be

$$\Delta x \leq (1/N_\lambda)(V/f) \tag{2}$$

where V is the minimum velocity of interest and f is the maximum frequency (in hertz) of interest.

A very early study (Ref. 6) had recommended $N_\lambda = 25$ with box ARs of the order of unity, and another study (Ref. 7) has recommended $N_\lambda = 18$ up to a Mach number of 0.75 with more boxes at higher Mach numbers (e.g., 24 at Mach 0.80, 34 at Mach 0.85, and 54 at Mach 0.9).

Since the problem size depends on the number of boxes, it is important to use the minimum number that will provide acceptable results. The situation is further complicated by confusion regarding the criteria that were used to establish the guidelines. This paper attempts to establish new guidelines for the enhanced DLM as implemented in the computer program N5KQ. The rigid AGARD wing/tail example of Ref. 3 is reconsidered at higher reduced frequencies and Mach numbers and with different aerodynamic modeling, both chordwise and spanwise. By numerical experimentation, the minimum number of box chords per wavelength is investigated (relative to Ref. 6); then the maximum AR of the boxes is further investigated (relative to Ref. 3). The next examples are two rectangular wings, used to study the effect of AR. The first has an AR of 2.0 and is divided into 20 strips with a varying number of chordwise boxes up to 100. The second wing is divided into 20 strips with 20 chordwise boxes and the wing span is extended to vary the box ARs from 1 to 10. A complete flexible airplane example, representative of a large business aircraft, is selected to study the effects of aerodynamic modeling on the generalized aerodynamic forces in typical vibration modes of bending and torsion, and finally, the LANN wing is selected to examine convergence of flexible-mode generalized aerodynamic forces.

Applications

Wing/horizontal stabilizer combination. This configuration is one of those proposed by the AGARD Structures and Materials Panel for comparison of numerical interfering lifting-surface theories. The coplanar configuration is shown in Fig. 1.

Limited calculations at a Mach number of $M = 0.8$ were presented in Ref. 6 in the first attempt to determine the chordwise requirements for convergence of the DLM. (The same models were reconsidered in Ref. 3.) It was assumed in Ref. 6 that

Received 7 October 1997; revision received 28 January 1999; accepted for publication 4 March 1999.

*Consulting Engineer; billrodden@aol.com.
†Technical Specialist, Loads and Dynamics; ptaylor@gulfaero.com. Associate Fellow AIAA.
‡Consulting Engineer; mcintosh@aimnet.com. Associate Fellow AIAA.
§Senior Engineer/Scientist, Loads and Dynamics; myles.l.baker@boeing.com. Member AIAA.

convergence had been achieved with 12 strips with 12 chordwise boxes on the wing and 10 chordwise boxes on the tail, giving a total of 264 boxes (the largest problem considered in the paper and an extremely large problem for the time). At the reduced frequency of $k = \omega s/V = 1.5$ ($k_r = \omega\bar{c}/2V = 1.2$, where $s = 1.0$ is the semispan and $\bar{c} = 1.6$ is the reference chord), the wavelength was $\lambda = 4.189$ ($\lambda/s = \pi/k$). The box chord at the wing root was $0.188 = 0.0448\lambda$, and this led to the guideline that chordwise box sizes should be no greater than $\frac{1}{25}$ of the wavelength or $N_\lambda = 25$. Had the box chord length at midspan (0.133) been compared with the wavelength ($0.133 = 0.0318\lambda$), a guideline of 30 boxes per wavelength would have been recommended. Larger models are considered here. Two sets of spanwise divisions have 12 strips (divided at 0.1, 0.2, 0.3, 0.4, 0.5, 0.6, 0.7, 0.77, 0.84, 0.91, and 0.965 fractions of the span) and 8 strips (divided at $\frac{1}{6}$, $\frac{1}{3}$, $\frac{1}{2}$, $\frac{2}{3}$, $\frac{5}{6}$, 0.9, and 0.96 fractions of the span). The present convergence study considers the following number of equal fraction chord boxes on the coplanar wing and tail, respectively: 8 and 4, 10 and 6, 14 and 8, 18 and 10, 22 and 12, 26 and 14, and 30 and 16. The 12 strips and the 8 strips were the same for all combinations of boxes, so the total number of boxes for the various cases for 12 strips were 144, 192, 264, 336, 408, 480, and 552, and for 8 strips were 96, 128, 176, 224, 272, 320, and 368. The lift coefficient C_L (based on the wing area $S_w = 3.2$) for oscillatory plunging with unit amplitude h_0/s is shown in Tables 1–3 in the form of $C_L/ik(h_0/s)$ for the various numbers of boxes. The monotonic convergence is seen in perusals of the three tables. However, the case of 264 boxes had not converged (to three significant figures) as seen in the present calculations in Table 1, but 552 boxes may be sufficiently converged. The 552 box case has 30 chordwise boxes on the wing, a box chord of 0.0533 at midspan, and this is $\frac{1}{80}$th of the wavelength.

Table 1 AGARD wing/tail configuration: comparison of lift coefficients for plunging $C_L/ik(h_0/s)$, with varying number of strips and $k_r = 1.2$, $M = 0.80$

Boxes[a]	N5KQ	N5KA	Boxes[b]	N5KQ
$144\left(\frac{8}{4}\right)$[c]	3.863 $+i3.002$	4.054 $+i3.005$	$96\left(\frac{8}{4}\right)$	3.965 $+i2.993$
$192\left(\frac{10}{6}\right)$	4.045 $+i2.980$	4.250 $+i2.980$	$128\left(\frac{10}{6}\right)$	4.164 $+i2.992$
$264\left(\frac{14}{8}\right)$	4.207 $+i2.982$	4.345 $+i2.974$	$176\left(\frac{14}{8}\right)$	4.308 $+i2.987$
$336\left(\frac{18}{10}\right)$	4.307 $+i2.988$	4.382 $+i2.970$	$224\left(\frac{18}{10}\right)$	4.365 $+i2.973$
$408\left(\frac{22}{12}\right)$	4.363 $+i2.984$	4.408 $+i2.967$	$272\left(\frac{22}{12}\right)$	4.396 $+i2.961$
$480\left(\frac{26}{14}\right)$	4.394 $+i2.976$	4.426 $+i2.964$	$320\left(\frac{26}{14}\right)$	4.417 $+i2.965$
$552\left(\frac{30}{16}\right)$	4.413 $+i2.911$	4.436 $+i2.962$	$368\left(\frac{30}{16}\right)$	4.432 $+i2.964$

[a] 12 strips.
[b] 8 strips.
[c] $144\left(\frac{8}{4}\right)$ denotes 8 equal chordwise divisions on the wing and 4 on the tail with a total of 144 boxes.

Applying this new guideline of 80 boxes per wavelength for three-significant-figure convergence at lower reduced frequencies requires 15 boxes at $k_r = 0.6$ (the 264-box case appears to be converged) and requires 8 boxes at $k_r = 0.3$ [the 192-box case (10 chordwise boxes) is also converged].

The effect of Mach number is studied in Table 3 at four Mach numbers from 0.60 to 0.95. A perusal of the tabulated results does not indicate any dependence of the rate of convergence on the Mach number, as had been proposed in Ref. 7.

A requirement for three-significant-figure convergence seems rather extreme in view of the past successes of the DLM, so a new criterion for only two-figure convergence might be more appropriate.

Table 2 AGARD wing/tail configuration: comparison of lift coefficients for plunging $C_L/ik(h_0/s)$, with varying reduced frequency and $M = 0.80$, 12 strips

Boxes	$k_r = 0.3$	$k_r = 0.6$	$k_r = 1.2$	$k_r = 2.4$
$144\left(\frac{8}{4}\right)$	2.163 $+i1.153$	2.671 $+i2.068$	3.863 $+i3.002$	4.715 $+i2.986$
$192\left(\frac{10}{6}\right)$	2.174 $+i1.157$	2.716 $+i2.075$	4.045 $+i2.980$	5.155 $+i2.808$
$264\left(\frac{14}{8}\right)$	2.182 $+i1.159$	2.751 $+i2.081$	4.207 $+i2.982$	5.656 $+i2.659$
$336\left(\frac{18}{10}\right)$	2.186 $+i1.160$	2.770 $+i2.086$	4.307 $+i2.988$	5.993 $+i2.526$
$408\left(\frac{22}{12}\right)$	2.189 $+i1.161$	2.781 $+i2.087$	4.363 $+i2.984$	6.148 $+i2.409$
$480\left(\frac{26}{14}\right)$	2.190 $+i1.161$	2.787 $+i2.088$	4.394 $+i2.976$	6.214 $+i2.338$
$552\left(\frac{30}{16}\right)$	2.191 $+i1.161$	2.791 $+i2.088$	4.413 $+i2.911$	6.252 $+i2.294$

Table 3 AGARD wing/tail configuration: comparison of lift coefficients for plunging $C_L/ik(h_0/s)$, with varying Mach number and $k_r = 1.2$, 12 strips

Boxes	$M = 0.60$	$M = 0.80$	$M = 0.90$	$M = 0.95$
$144\left(\frac{8}{4}\right)$	3.433 $+i3.374$	3.863 $+i3.002$	3.986 $+i2.691$	4.010 $+i2.567$
$192\left(\frac{10}{6}\right)$	3.573 $+i3.402$	4.045 $+i2.980$	4.155 $+i2.621$	4.167 $+i2.472$
$264\left(\frac{14}{8}\right)$	3.693 $+i3.435$	4.207 $+i2.982$	4.334 $+i2.590$	4.376 $+i2.422$
$336\left(\frac{18}{10}\right)$	3.770 $+i3.458$	4.307 $+i2.988$	4.444 $+i2.585$	4.512 $+i2.421$
$408\left(\frac{22}{12}\right)$	3.819 $+i3.471$	4.363 $+i2.984$	4.490 $+i2.564$	4.550 $+i2.387$
$480\left(\frac{26}{14}\right)$	3.849 $+i3.477$	4.394 $+i2.976$	4.502 $+i2.547$	4.539 $+i2.365$
$552\left(\frac{30}{16}\right)$	3.867 $+i3.481$	4.413 $+i2.911$	4.507 $+i2.535$	4.527 $+i2.353$

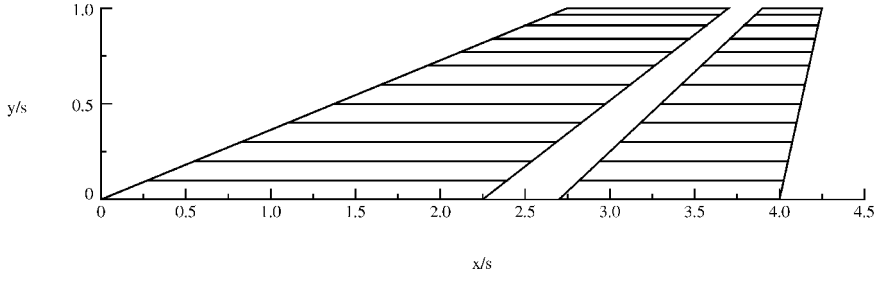

Fig. 1 AGARD wing/horizontal tail configuration.

However, Table 2 suggests that at least 50 boxes per wavelength would be required.

Rectangular wings. The effect of box AR is studied on rectangular wings pitching about their midchord at $M = 0.8$. The first wing has AR = 2 and is divided into 10 equal-width strips. The strips are divided into equal chord boxes from 5 to 100. The box ARs vary from 0.5 to 10.0. The reduced frequency dependence is also varied from $k_r = 0.1$ to 2.0. The results for lift coefficient C_L are shown in Table 4 for the four frequencies of $k_r = 0.1$, 0.5, 1.0, and 2.0. The effect of box AR is not observed, and both the real and the imaginary parts seem to have converged for the same number of chordwise boxes at each reduced frequency for both N5KA and N5KQ, in contrast to the previous recommendation to limit the AR to 3. Table 4 suggests no limit on box ARs (up to 10). Furthermore, the real parts between N5KA and N5KQ are also in reasonable agreement. However, a significant difference is found between the imaginary parts at the high frequencies of $k_r = 1.0$ and 2.0, and it is shown below that N5KQ gives a more accurate estimate than N5KA for the aerodynamic damping.

Table 4 Rectangular AR = 2 wing: comparison of lift coefficients for pitching with varying number of chordwise boxes and $M = 0.8$, 10 strips

	Chordwise	N5KQ		N5KA	
k_r	boxes	Real	Imaginary	Real	Imaginary
0.1	5	2.968	0.3626	2.968	0.3626
0.1	10	2.968	0.3565	2.975	0.3653
0.1	20	2.971	0.3563	2.977	0.3657
0.1	50	2.972	0.3560	2.978	0.3658
0.1	100	2.972	0.3560	2.978	0.3658
0.5	5	3.638	1.739	3.638	1.739
0.5	10	3.770	1.724	3.810	1.731
0.5	20	3.859	1.712	3.870	1.724
0.5	50	3.898	1.706	3.885	1.723
0.5	100	3.902	1.705	3.887	1.722
1.0	5	4.492	1.823	4.492	1.823
1.0	10	4.768	1.528	4.820	1.479
1.0	20	4.901	1.313	4.920	1.338
1.0	50	4.948	1.212	4.930	1.303
1.0	100	4.953	1.200	4.932	1.300
2.0	5	4.652	2.380	4.652	2.380
2.0	10	5.396	1.814	5.461	1.729
2.0	20	5.720	1.393	5.681	1.449
2.0	50	5.840	1.194	5.730	1.378
2.0	100	5.854	1.170	5.735	1.371

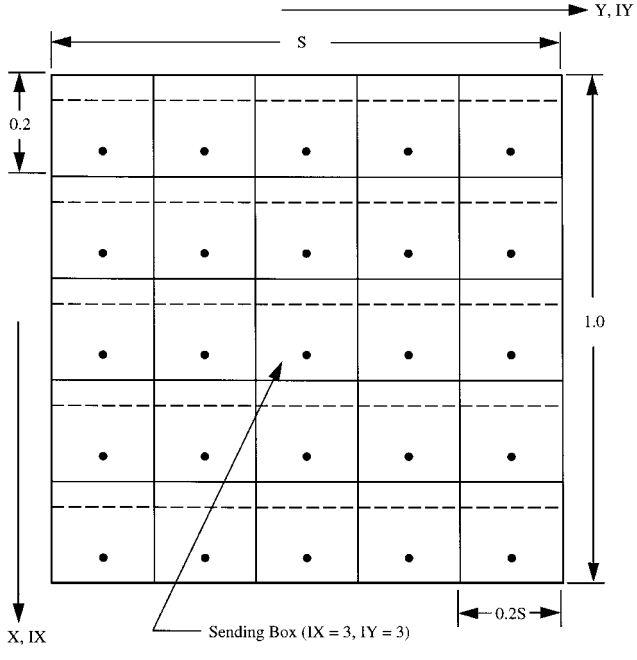

Fig. 2 Layout used for box AR comparisons.

To examine the question of aerodynamic damping, we compare incremental oscillatory kernel functions for a 5×5 grid of boxes. The box chords are fixed at 0.2 units, and the box spans are varied to produce different box ARs. The reference chord $\bar{c}$ is varied to produce the desired number of chordwise boxes. The layout is illustrated in Fig. 2; note that the sending box is taken to be the central one, identified by the location parameters $IX = 3$, $IY = 3$. To meet the criterion of 50 boxes per wavelength for $k_r = 2.0$, a

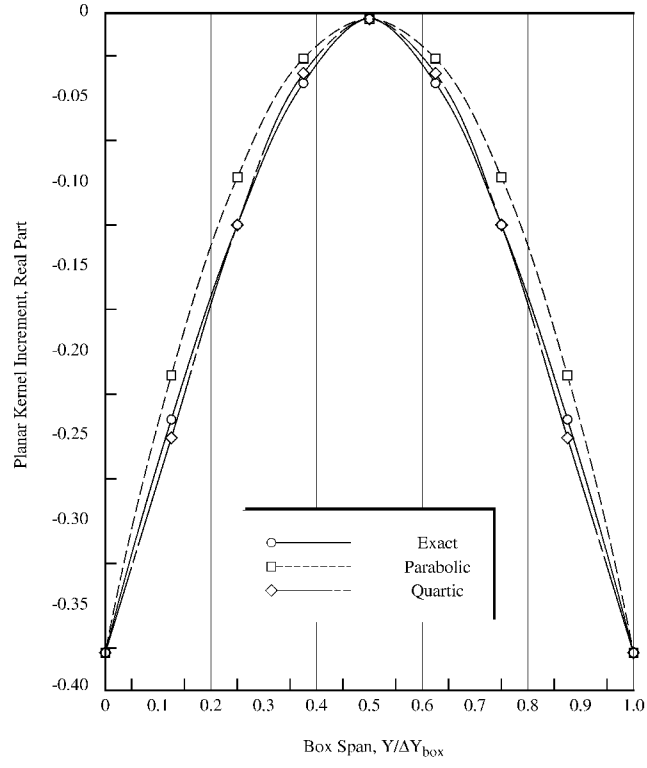

Fig. 3 Comparison of real part of planar kernel numerator increment; box AR = 10.0.

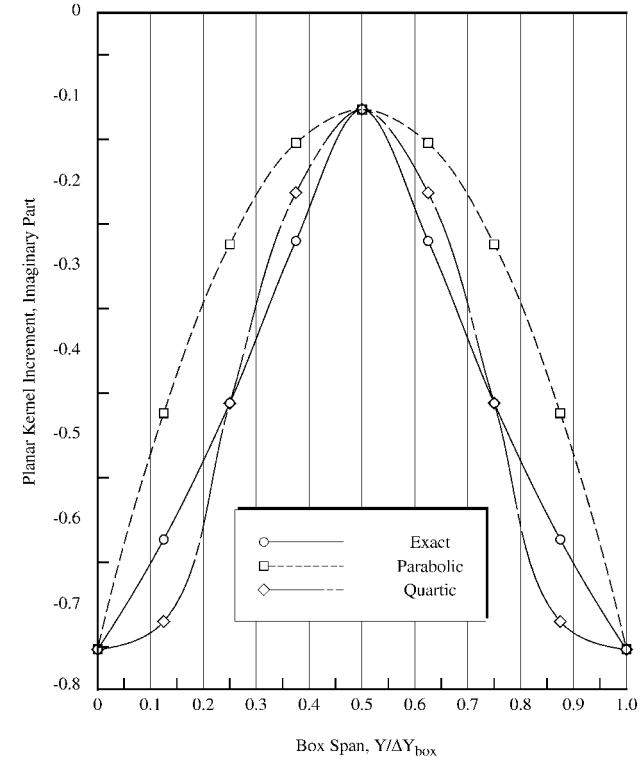

Fig. 4 Comparison of imaginary part of planar kernel increment numerator; box AR = 10.0.

reference chord of 7.0 is chosen, which gives 35 as the number of chordwise boxes (NC) ($NC = 35$). Figures 3 and 4 present comparisons of the real and the imaginary parts, respectively, of the planar kernel increment for identical sending and receiving boxes. The box ARs, equal to the spanwise grid width S, are 10. The Mach number is 0.8. The quartic approximation is superior to the parabolic approximation, in particular, for the imaginary part. Since the doublet-lattice solution involves integrating the kernel functions over the box spans, the areas under the curves are a truer measure of approximation errors, and it is seen that the quartic errors tend to be self-canceling. Data for receiving boxes directly in front of and behind the sending box, i.e., in the $IY = 3$ column, yield similar conclusions. As the distance between the receiving and sending boxes increases, both parabolic and quartic approximations become more accurate. These results suggest that the previous AR limit of 3.0 for N5KA is reasonable and box ARs higher than 10.0 should be avoided with N5KQ.

The second study of the box AR is on rectangular wings, now divided into 20 equal-width strips having 20 equal chord boxes. Here the box ARs are increased from 1 to 10 by an increase in the span so that the wing AR varies from 2 to 20. The same four reduced frequencies are considered, and the results are shown in Table 5. Again, the significant results are found in more accurate imaginary parts; the effect of the AR on the real parts is secondary.

Representative jet aircraft. Generalized aerodynamic forces (GAFs) were calculated for a representative jet aircraft. The structure is modeled as a series of beams representing the elastic axis of each component and the distributed mass of the aircraft is modeled as lumped masses. The aerodynamic model (shown in Fig. 5) consists of panels representing the wing and winglet and the horizontal tail. For simplicity, the fuselage aerodynamic modeling was ignored, as were the nacelles. The wing has 10 chordwise and 19 spanwise boxes on each side, and each winglet has 10 chordwise and 11 spanwise boxes. The horizontal tail has 11 chordwise and 10 spanwise boxes, for a total model of 410 boxes. GAFs were calculated by use of MSC/NASTRAN and by outputting the matrices designated as QHH by means of a DMAP ALTER. The Mach number is $M = 0.5$, and the reduced frequencies are $k_r = 0.01, 0.06, 0.12, 0.2, 0.5, 1.0, 2.0$, and 3.0. The plots of selected structural mode shapes are shown in Figs. 6–8. Mode 10 (Fig. 6) has significant horizontal stabilizer and elevator motion, while modes 16 (Fig. 7) and 25 (Fig. 8) have significant winglet bending as well as aileron motion.

Plots of the diagonal elements of the GAF matrices for the selected modes are shown in Figs. 9–11, respectively. The symbols are points calculated at the list of reduced frequencies mentioned in the preceding paragraph, while the lines are a spline similar to that

Table 5 Rectangular wing: comparison of lift coefficients for pitching with varying wing ARs, $M = 0.8$, 20 chordwise boxes, 20 strips

	Box	N5KQ		N5KA		Wing
k_r	AR	Real	Imaginary	Real	Imaginary	AR
0.1	1	2.908	0.3546	2.915	0.3653	2
0.1	2	4.587	−0.0370	4.608	−0.0186	4
0.1	3	5.414	−0.5164	5.445	−0.4964	6
0.1	5	6.038	−1.166	6.078	−1.144	10
0.1	10	6.342	−1.691	6.392	−1.649	20
0.5	1	3.775	1.709	3.814	1.735	2
0.5	2	4.701	0.5339	4.726	0.5393	4
0.5	3	4.747	0.2547	4.740	0.2891	6
0.5	5	4.873	0.0507	4.825	0.1560	10
0.5	10	4.933	−0.0355	4.843	0.2070	20
1.0	1	4.832	1.335	4.897	1.291	2
1.0	2	4.874	0.9398	4.882	0.9511	4
1.0	3	4.921	0.7556	4.906	0.8530	6
1.0	5	4.989	0.6529	4.947	0.9123	10
1.0	10	5.026	0.7201	4.888	1.272	20
2.0	1	5.610	1.432	5.647	1.355	2
2.0	2	5.800	0.9705	5.770	1.034	4
2.0	3	5.856	0.8407	5.775	1.091	6
2.0	5	5.878	0.8073	5.681	1.368	10
2.0	10	5.806	1.0623	5.150	2.257	20

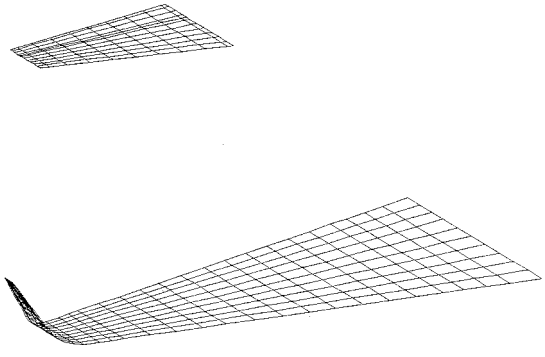

Fig. 5 Jet aircraft aerodynamic representation.

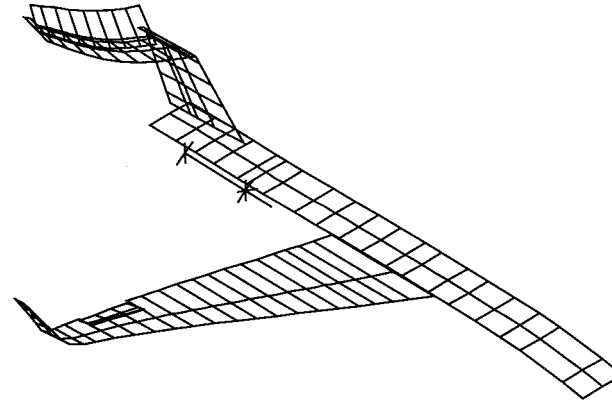

Fig. 6 Jet aircraft, structural mode 10.

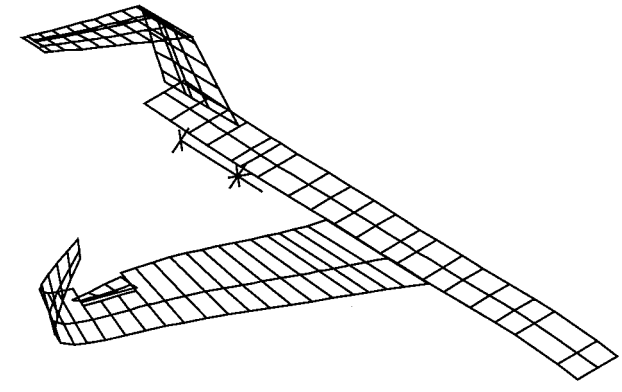

Fig. 7 Jet aircraft, structural mode 16.

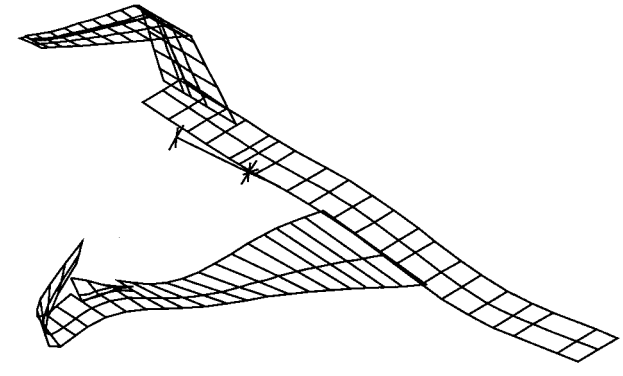

Fig. 8 Jet aircraft, structural mode 25.

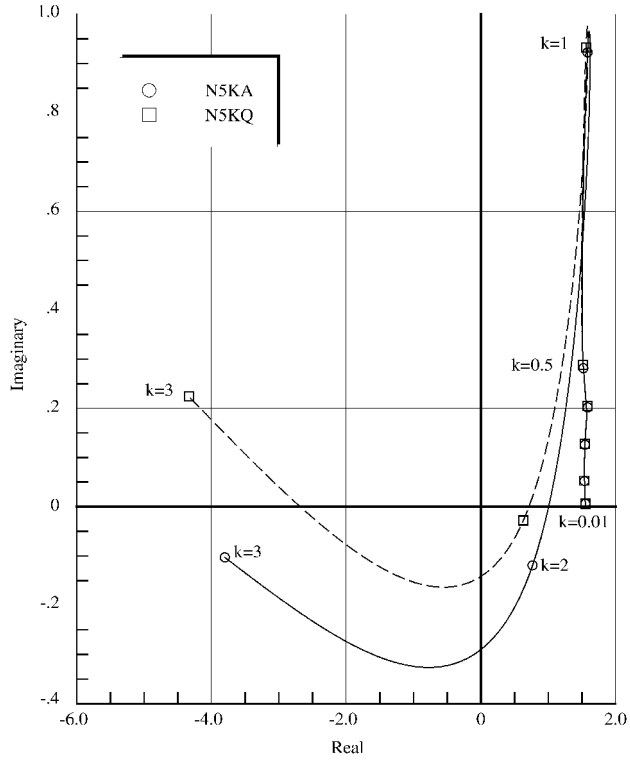

Fig. 9 Jet aircraft, GAF in mode 10 due to mode 10.

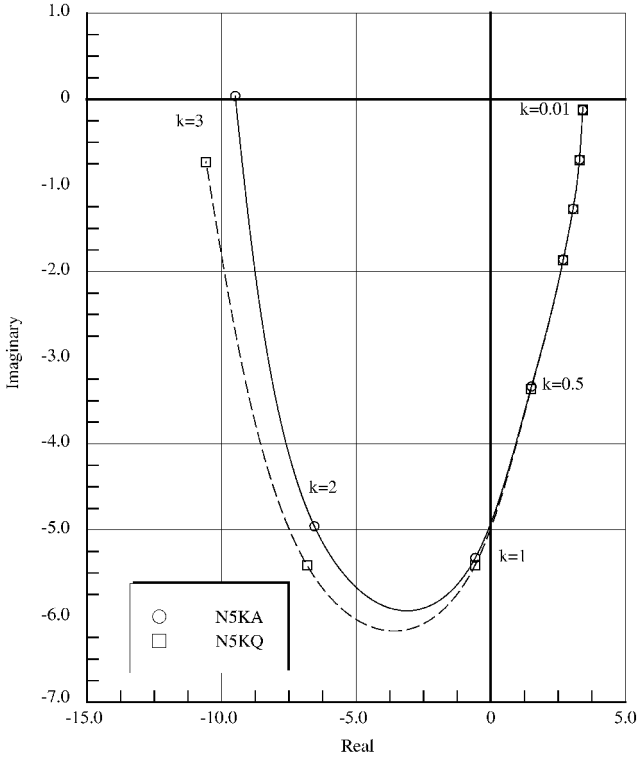

Fig. 10 Jet aircraft, GAF in mode 16 due to mode 16.

used in MSC/NASTRAN for interpolating the aerodynamic forces for different k_r.

Figure 9 shows interesting generalized force behavior for mode 10. The plot starts at a k_r of 0.01 on the positive real axis. As the reduced frequency is increased, the real part remains constant, while the imaginary part grows. At a reduced frequency of 1.0, both the real and the imaginary parts then start decreasing, until a reduced frequency of a little more than 2.0 is reached, at which point the

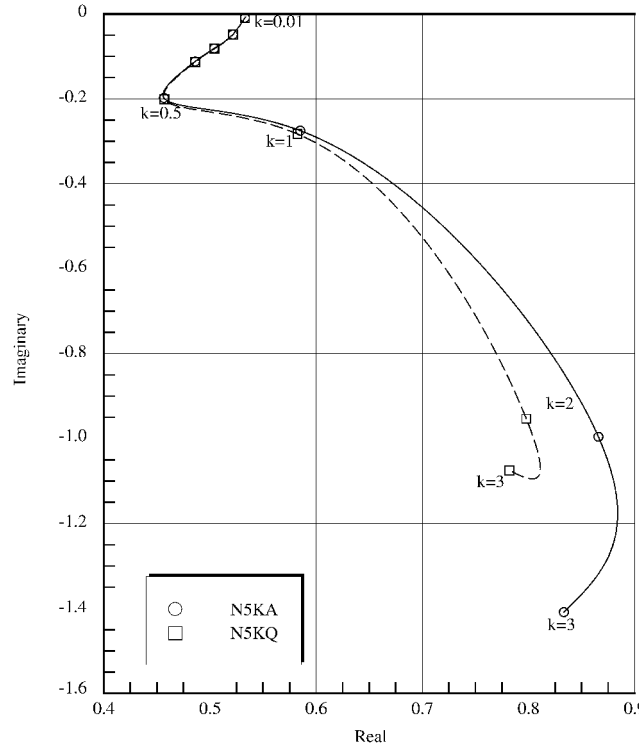

Fig. 11 Jet aircraft, GAF in mode 25 due to mode 25.

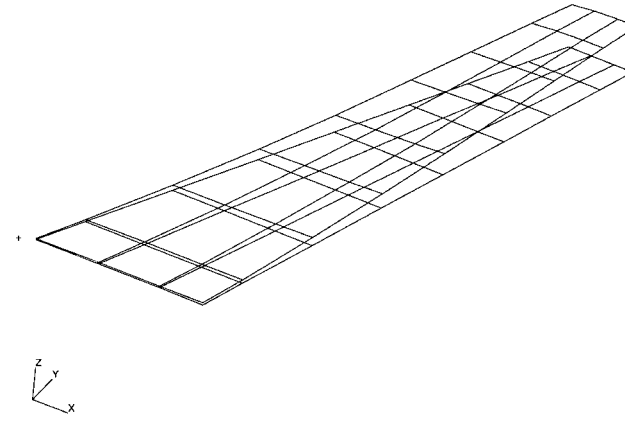

Fig. 12 LANN wing, structural mode 1.

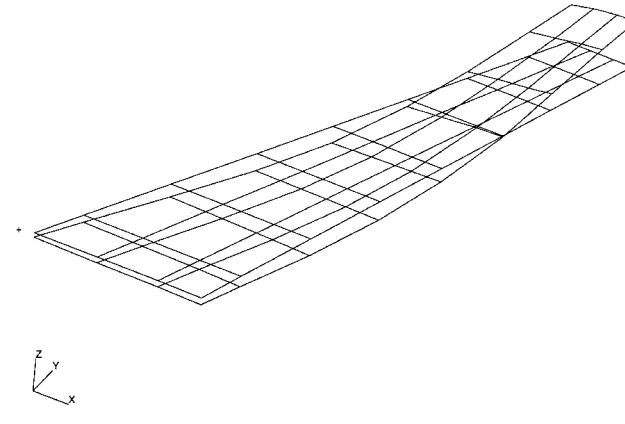

Fig. 13 LANN wing, structural mode 2.

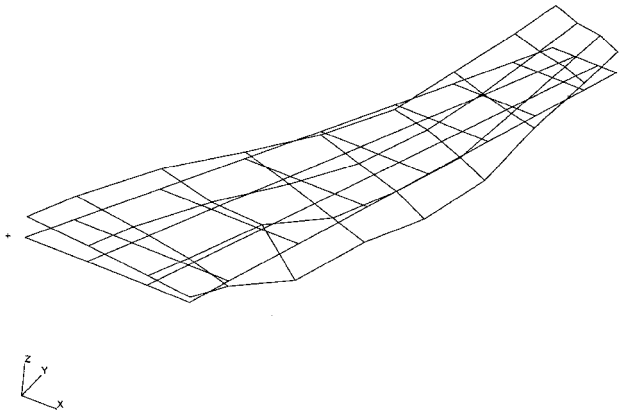

Fig. 14 LANN wing, structural mode 3.

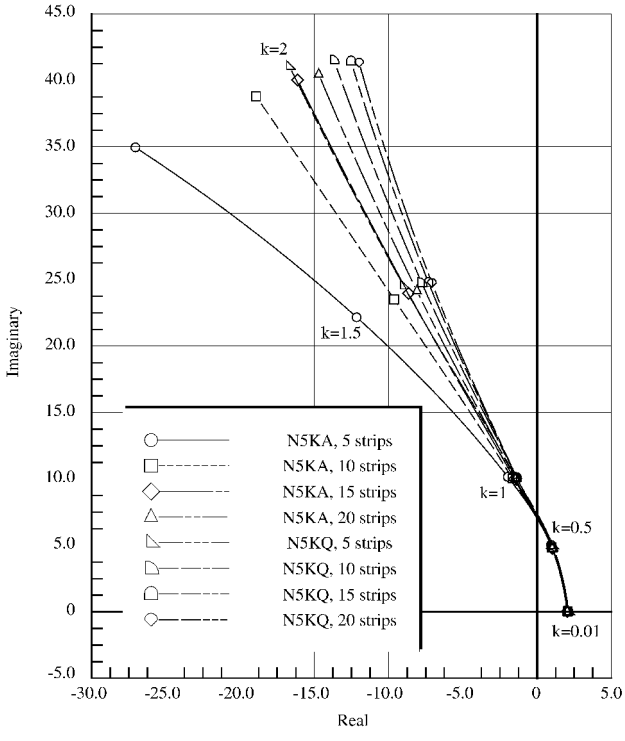

Fig. 15 LANN wing, GAF in mode 1 due to mode 1.

imaginary part once again starts increasing. It is believed that this behavior is caused by the coupling between elevator rotation and horizontal tail bending motion.

The generalized forces show good correlation up to a reduced frequency of 1.0 even for the complex modal deflections; however, above 1.0, the deviation is quite obvious and in some instances has the opposite sign (e.g., in Fig. 9).

LANN wing. Another convergence study uses a high-AR wing representative of a subsonic transport wing. To perform pure convergence studies, a clean wing configuration is required for giving the necessary flexibility in dividing the wing into many boxes. For this purpose, the LANN wing (Ref. 8) was selected.

Analyses were run to generate the first seven GAFs that were due to the first seven modes of the wing at a Mach number of 0.8 and reduced frequencies ranging from 0.0 to 2.0.

Various combinations of chordwise and spanwise divisions were used, ranging from 5 chordwise and 5 spanwise divisions to 25 chordwise and 20 spanwise divisions. In this example, the convergence behavior between N5KA and N5KQ was not much different as the number of chordwise boxes was increased, but the spanwise behavior was significantly different.

An investigation of the steady case, i.e., the vortex-lattice method (VLM) to which the DLM reduces at zero reduced frequency, has shown slow convergence as the number of strips is increased. This has been observed in the past by Hough,[9,10] who obtained improved convergence by following a suggestion of Rubbert[11] that equally spaced lattices on a surface should be inset from the tip by a fraction d of the lattice span ($0 < d < 1$). Hough observed that $d = \frac{1}{4}$ dramatically improves the convergence. It should be noted that Hough's argument leading to $d = \frac{1}{4}$ is based on a symmetrical (elliptical) loading in the steady case. Limited calculations to date indicate that the tip correction also improves the antisymmetric and oscillatory cases and will be reported subsequently.

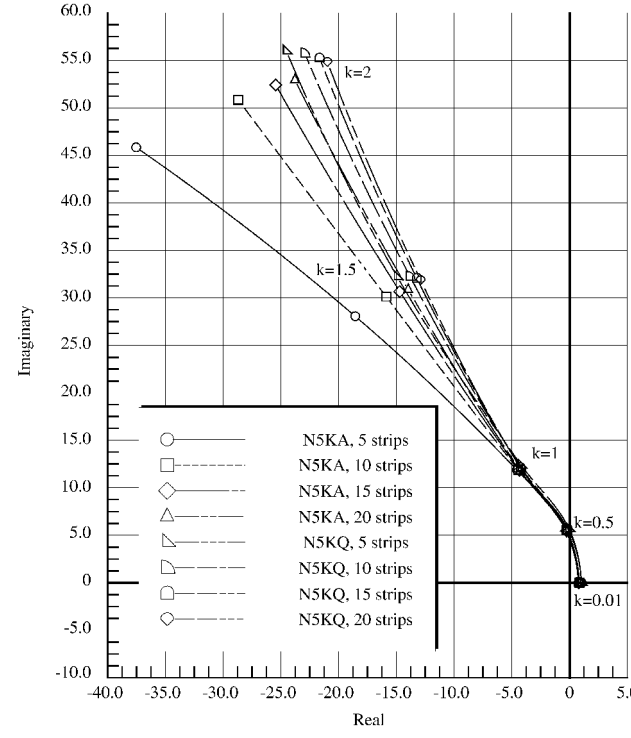

Fig. 16 LANN wing, GAF in mode 2 due to mode 2.

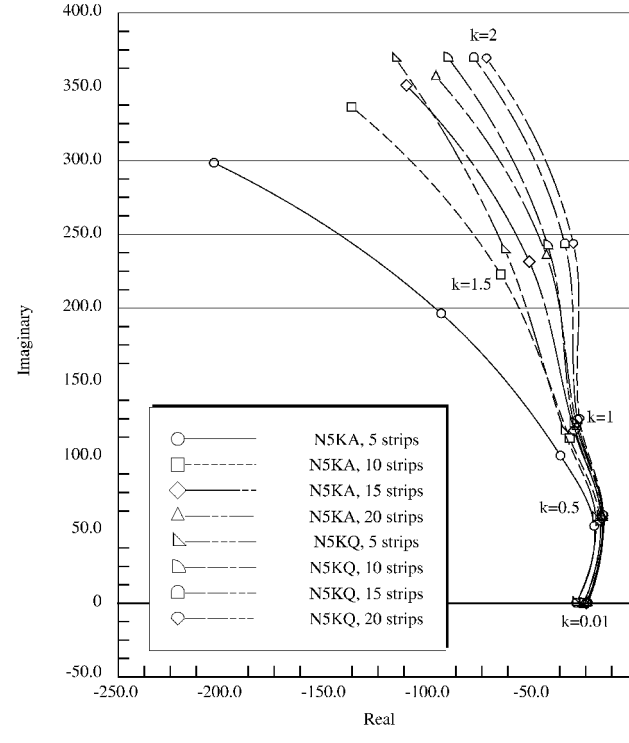

Fig. 17 LANN wing, GAF in mode 3 due to mode 3.

The first three vibration modes of the LANN wing are shown in Figs. 12–14, and the first three diagonal elements of the GAF matrix are shown in Figs. 15–17. In each GAF plot, the term is plotted in the complex plane for reduced frequencies between 0.0 and 2.0. The results from the present method (labeled N5KQ) and Ref. 4 (labeled N5KA) are each plotted for 5, 10, 15, and 20 spanwise strips.

While close convergence was not obtained at the higher reduced frequencies, the improvement of N5KQ relative to N5KA can clearly be seen. If one extrapolates the convergence trend indicated by the results from N5KA to estimate the converged solution, it becomes obvious that for similar numbers of spanwise divisions N5KQ is much closer to the converged solution. In fact, a general trend appears in the diagonal GAF entries, in which N5KQ with only 5 spanwise strips gives results comparable with those of N5KA with 15 spanwise divisions. This indicates that N5KQ can offer significant computational savings over N5KA. Depending on the reduced frequency range of interest and the required convergence level, it may be possible to reduce the number of required spanwise strips by a factor of 2 or 3. Conversely, if the total number of boxes is limited by software or computing time constraints, the current method can offer results significantly closer to the converged solution without increasing the problem size.

Conclusions

The convergence characteristics of the enhanced DLM (N5KQ) have been investigated further beyond the studies of Ref. 3. The present studies have shown no significant Mach number effect, as suggested elsewhere.[7] Furthermore, box aspect ratio, previously proposed to be less than 3, appears to be accurate perhaps up to 10. However, one of the present studies has also indicated that 50 chordwise boxes per wavelength may be required for achieving convergence of force coefficients to two significant figures. This is a substantial increase in the $N_\lambda = 12, 18$, or 25 boxes variously recommended elsewhere[5–7] and warrants further study on other configurations as well as in flutter and gust response analyses.

Since the generation of an unsteady aerodynamic model for flutter and gust analyses typically occurs early in the design cycle of an aircraft, even during design by optimization methods (and the aerodynamic configuration is always defined well before the structure is optimized), it is important to have the most accurate aerodynamic loads available. The quartic approximation of N5KQ allows increased accuracy for a given model size, as demonstrated by the convergence studies presented here and in Ref. 3.

The computer program N5KQ is available from the authors and is also available in MSC/NASTRAN, Ver. 70.5.

Acknowledgment

This paper was presented at the Confederation of European Aerospace Societies International Forum on Aeroelasticity and Structural Dynamics, Rome, 17–20 June 1997.

References

[1] Albano, E., and Rodden, W. P., "A Doublet-Lattice Method for Calculating Lift Distributions on Oscillating Surfaces in Subsonic Flows," *AIAA Journal,* Vol. 7, No. 2, 1969, pp. 279–285.

[2] Giesing, J. P., Rodden, W. P., and Kálmán, T. P., "Refinement of the Nonplanar Aspects of the Subsonic Doublet-Lattice Lifting Surface Method," *Journal of Aircraft*, Vol. 9, No. 1, 1972, pp. 69–73.

[3] Rodden, W. P., Taylor, P. F., and McIntosh, S. C., Jr., "Further Refinement of the Nonplanar Aspects of the Subsonic Doublet-Lattice Lifting Surface Method," *Journal of Aircraft*, Vol. 35, No. 5, 1998, pp. 720–727.

[4] Giesing, J. P., Kálmán, T. P., and Rodden, W. P., "Subsonic Unsteady Aerodynamics for General Configurations: Part II—Application of the Doublet-Lattice Method and the Method of Images to Lifting-Surface/Body Interference," U.S. Air Force Flight Dynamics Lab., Rept. AFFDL-TR-71-5, Pt. II, Dayton, OH, April 1972.

[5] Rodden, W. P., and Johnson, E. H., *MSC/NASTRAN Aeroelastic Analysis User's Guide*, MacNeal-Schwendler Corp., Los Angeles, 1994.

[6] Rodden, W. P., Giesing, J. P., and Kálmán, T. P., "New Developments and Applications of the Subsonic Doublet-Lattice Method for Nonplanar Configurations," *Symposium on Unsteady Aerodynamics for Aeroelastic Analyses of Interfering Surfaces*, Paper 4, AGARD-CP-80-71, 1970.

[7] Giesing, J. P., McGrew, J. A., Smith, M. K., Fujita, S. S., Britt, R. T., Chai, Y. K., and Glade, T. W., "Modifications to the VIBRA-6 Nuclear Blast Response Computer Program," U.S. Air Force Weapons Lab., Rept. AFWL-TR-81-166, Pt. 1, Dayton, OH, Aug. 1983, p. 176.

[8] Horsten, J. J., den Boer, R. G., and Zwaan, R. J., "Unsteady Transonic Pressure Measurements on a Semispan Wind Tunnel Model of a Transport-Type Supercritical Wing (LANN Model), Part I," U.S. Air Force Wright Aeronautical Lab., Rept. AFWAL-TR-83-3039, Dayton, OH, March 1983.

[9] Hough, G. R., "Remarks on Vortex-Lattice Methods," *Journal of Aircraft*, Vol. 10, No. 5, 1973, pp. 314–317.

[10] Hough, G. R., "Lattice Arrangement for Rapid Convergence," *Vortex-Lattice Utilization*, NASA SP-405, May 1976, pp. 325–342.

[11] Rubbert, P. E., "Theoretical Characteristics of Arbitrary Wings by a Non-Planar Vortex Lattice Method," The Boeing Co., D6-9244, Renton, WA, 1964.